Comparative Biochemistry and Physiology, Part A 236 (2019) 110520

Contents lists available at ScienceDirect

Comparative Biochemistry and Physiology, Part A

journal homepage: www.elsevier.com/locate/cbpa

Deep-sea sharks: Relation between the liver's buoyancy and red aerobic muscle volumes, a new approach

Nicolas Pinte[a,*,1], Mathilde Godefroid[a,1], Ouissam Abbas[b], Vincent Baeten[b], Jérôme Mallefet[a]

[a] Marine Biology Laboratory, Earth and Life Institute, Catholic University of Louvain, 3 Place Croix du Sud, Building Kelner D-107, 1348 Louvain-la-Neuve, Belgium
[b] CRA-W, Department Value of the Production, Food and Feed Quality Unit, Building Maurice Henseval, Chaussée de Namur 24, 5030 Gembloux, Belgium

ARTICLE INFO

Keywords:
Squaliformes
Lipids
Liver
Muscle
FT-Raman
FT-MIR

ABSTRACT

Shark's buoyancy depends on two types of force: (i) the hydrostatic force which is mainly provided by their liver filled with low density lipids and (ii) the hydrodynamic force which is provided by the morphology of their body and fins. Shallow-water shark species are usually negatively buoyant, whereas deep-sea shark species have been suggested to display neutral buoyancy. It has been suggested that species that are close to the neutrality would have less red aerobic muscle fibers. Here, we investigated several liver features (the hepatosomatic index, the oil content and the lipid composition) playing a major role regarding the buoyancy of three deep-sea shark species (*Etmopterus molleri*, *Etmopterus spinax* and *Isistius brasiliensis*) and one shallow-water counterpart (*Galeus melastomus*). We used FT-Raman and FT-MIR spectroscopy to qualify/quantify the lipid composition of their liver. Our results showed that most deep-sea shark species studied have liver features providing more buoyancy than their shallow-water counterparts, appart from *E. molleri* which shows liver's features that resemble more shallow-water shark species (e.g. *G. melastomus*). Finally, data regarding liver features of several deep-sea shark species from the literature were added and the red aerobic muscle distribution/proportion of nine species was measured, to reveal how these parameters might be related. Our results showed that sharks characterized by a liver providing more hydrostatic force possess proportionally less red aerobic muscles than sharks having a liver that contributes less to their buoyancy. Therefore, our results i.e. deep-sea shark displaying less red aerobic muscle with a liver providing more buoyancy, support low metabolic rates hence slow swimming speed.

1. Introduction

The buoyancy of marine organisms remains an essential feature to their locomotion, it also explains the distribution of species across the different marine and fresh water environments. Buoyancy (positive, negative or neutral) can constitute a good compromise to reduce the energy expenditure during locomotion. For example, the sperm whales use their spermaceti to deep dive at lower energy costs (Clarke et al., 1984), most fishes use a swim bladder to adjust their buoyancy and ease their 3D-locomotion provided by their fins (Phleger, 1998). As regards to sharks, their buoyancy depends on two types of force: the hydrodynamic force is provided by the shape of the body and the fins; and the hydrostatic force depends on the density of the body, that is mainly influenced by the liver of sharks, also previously called the hydrostatic organ (Treberg and Speers-Roesch, 2016). Although previously mentioned in the literature as hydrodynamic and hydrostatic lifts due to the lift they provide to the whole shark body, in this paper, we will refer to the terms hydrostatic and hydrodynamic force. Other tissues may also act on the buoyancy of the shark's body but their implications on the buoyancy remains equivalent/vary less across species, compared to the role played by the liver (Malins et al., 1965; Sargent et al., 1972; Treberg and Speers-Roesch, 2016).

The relative proportion of the elasmobranch liver, measured through the hepatosomatic index (HSI; the liver weight divided by the body weight) is greater than for other marine organisms, it represents between 10 and 30% of the total body mass for sharks (Corner et al., 1969; Pethybridge et al., 2010; Nakamura et al., 2015). On top of that, the skeleton of sharks is cartilaginous and thus less dense than calcified skeletons (Bone and Moore, 2008). Therefore, the main factors affecting the hydrostatic force are (i) the mass of the liver, (ii) its oil content (OC) and (iii) the lipid classes in the oil and their respective densities (Shadwick et al., 2016). The shark liver oil is obtained through different lipid extractions. The percentage of OC ranges from 36 to 83% between species (Wetherbee and Nichols, 2000; Pethybridge et al., 2010). Four

* Corresponding author.
E-mail address: nicolas.pinte@uclouvain.be (N. Pinte).
[1] These authors contributed equally.

https://doi.org/10.1016/j.cbpa.2019.06.020
Received 12 February 2019; Received in revised form 26 June 2019; Accepted 26 June 2019
Available online 03 July 2019
1095-6433/ © 2019 Elsevier Inc. All rights reserved.

major lipid classes are mainly found in shark oil: the squalene (HC, hydrocarbon) which is the main hydrocarbon found in shark liver (Tsujimoto, 1916), the triacylglycerides (TAG), the diacylglycerides (DAGE) and the wax esters (WE) (Shadwick et al., 2016). All of them provide a specific hydrostatic force thanks to their respective densities which are lower than the surrounding seawater density (1.025 g/ml), in order of their relative contribution on the hydrostatic force: squalene (0.8562 g/ml), WE (0.8578 g/ml), DAGE (0.89 g/ml) and TAG (0.92 g/ml) (Bone and Moore, 2008; Shadwick et al., 2016). They also play a second function as ketone body source which acts as an energy reserve for the shark, apart from squalene that does not display evidences of these functions (Phleger, 1998; Bone and Moore, 2008; Watson and Dickson, 2015; Shadwick et al., 2016). Studies have shown that osmolytes may also contribute to the hydrostatic force (mainly trimethylamine N-oxyde [TMAO] and urea, for sharks) but that this contribution (around 10% of the liver contribution) is less important for deep-sea species than for shallow-water ones (Treberg and Speers-Roesch, 2016). Moreover, deep-sea shark species tend to have a greater proportion of TMAO than of urea and studies suggested that this accumulation by deep-sea animals may allow the protection of proteins against the destabilizing effects of high hydrostatic pressure (Yancey et al., 2018). Due to the minor role of osmolytes compared to liver features in the hydrostatic force, their contribution was not considered in this study.

Despite this, the buoyancy of shallow-water sharks is still believed as being negative. Indeed, several pelagic species display large pectoral fins that allow them to improve their hydrodynamic force by increasing their lift-drag ratio (Iosilevskii and Papastamatiou, 2016). Others, such as the hammerhead sharks, swim in a rolled manner so that the dorsal fin is approximately perpendicular to the gravity and provides a hydrodynamic force (Payne et al., 2016). Benthic sharks have a highly heterocercal caudal fin (dorsal lobe longer than ventral one), this shape also provides a hydrodynamic force in addition to the thrust (Thompson and Simanek, 1977; Shadwick and Goldbogen, 2012). In contrast, deep-sea shark species are known to be closer to neutral buoyancy (Bone and Roberts, 1969; Corner et al., 1969; Wetherbee and Nichols, 2000; Gleiss et al., 2017), as many of these sharks living in an oligotrophic environment display larger liver that contains higher oil content, richer in low-density lipids than their shallow-water counterparts. Neutral buoyancy would allow them to reduce their energy loss in such environment where food availability is low (Corner et al., 1969; Bakes and Nichols, 1995; Wetherbee and Nichols, 2000; Pethybridge et al., 2010). It has already been shown that the bluntnose sixgill shark (*Hexanchus griseus*) is characterized by positive buoyancy (Nakamura et al., 2015). However, it is important to note that no modelling of the sharks buoyancy has ever been made, implying that all papers to date built their conclusions on indirect measurements, without considering all the features playing a role in the buoyancy of the sharks (hydrostatic force, hydrodynamic force, tail beat, swimming speed, temperature of the surrounding environment, etc.).

The beat of the caudal fin of the shark is an important feature to consider. Indeed, most sharks have a heterocercal caudal fin providing force during each tailbeat (Thompson and Simanek, 1977; Shadwick and Goldbogen, 2012). This tail motion, taking part in the hydrodynamic force, is directly dependent on the composition of the shark's musculature. Fish muscles are present in higher proportion (40–60% of the total body mass) than for terrestrial vertebrates (20–40% of the total body mass) as they live and move in a denser environment (Bone, 1978). Sharks display two different types of muscle fibers: the white fibers, taking part during burst activities, are powered by the anaerobic metabolism and the red fibers, taking part during cruise swimming activities (main swimming mode used by the sharks) are powered by aerobic metabolism (Bone, 1966; Syme, 2005; Shadwick and Goldbogen, 2012; Shadwick et al., 2016). Bernal et al. in 2003 have shown that the red aerobic muscles distribution across the posterior part (25–95% of the fork length) is in higher proportion around 70% of the fork length (Bone, 1978; Bernal et al., 2003). They also evaluated the red aerobic muscles proportion being between 2 and 3% of the total body mass (Bernal et al., 2003). In 1966, Bone hypothesized that sharks that are close to neutral buoyancy should have fewer red aerobic muscle fibers. Indeed, it is difficult for marine organisms to swim slowly when they are negatively buoyant. For this reason and also to have high swimming capabilities, shallow-water sharks developed higher proportion of red aerobic muscle, whereas deep-sea sharks do not need a high proportion for their low swimming capabilities. While this hypothesis has been cited numerous times in the literature, it has never been directly tested through direct evidences (Shadwick and Goldbogen, 2012; Shadwick et al., 2016). Therefore, the study of deep-sea sharks, often suggested to be close to neutral buoyancy, should allow us to test this hypothesis.

In this work, we investigated the hydrostatic force provided by the liver of three deep-sea shark species (*Isistius brasiliensis*, *Etmopterus molleri* and *Etmopterus spinax*) and one shallow-water counterpart (*Galeus melanostomus*). For this purpose, we measured the HSI of the liver, its oil content (OC) and the diversity and abundance of the lipid classes within the liver oil through Fourier transform Raman (FT-Raman) and Mid-infrared (MIR) spectroscopy. We also completed our results with data from the literature, applying the liver hydrostatic force equation from Treberg and Speers-Roesch (2016) that characterizes the force provided by the liver. Finally, we measured the proportion of red aerobic muscles and described their distribution along the body of the studied species, aiming to correlate the total red aerobic muscle mass with the hydrostatic force provided by the liver and get a first experimental evidence supporting the hypothesis made by Bone in 1966.

2. Material and methods

2.1. Samples

The individuals *Etmopterus spinax* and *Galeus melastomus* were collected with deep longlines at ~220 m depth in the Raunefjord (Norway; 60.260623°N; 5.162056°E), during scientific surveys in January 2016 and February 2017. Specimens were then directly brought back to the Marine Research Field Station (Espegrend, Bergen University, Norway) and transferred into tanks maintained at 6 °C in a dark room. Sharks were euthanized following the local rules for experimental vertebrate care (Permit 12/14048). The liver was extracted and stored at −80 °C. The individuals *Etmopterus molleri* were caught by a longline at 500 m depth in the East China sea (Japan; 26.555543°N; 127.713359°E), in November 2016 and November 2017. Samplings and ethical procedures are similar than sharks from Norway. Finally, the individuals *Isistius brasiliensis* ($N = 6$) come from by-catch provided by fisherman from La Reunion island. Individuals were stored directly at −80 °C.

For each individual, the liver weight, total body weight, size of the body, sex and reproductive status were determined. The liver was collected for 44 samples: 13 *E. spinax*, 7 *G. melastomus*, 5 *I. brasiliensis* and 19 *E. molleri*.

In addition, other deep-sea shark species were collected only to obtain the red aerobic muscles quantification and distribution. These six other species (*Centrophorus squamosus*, *Deania calcea*, *Centroscymnus owstonii*, *Etmopterus granulosus, Dalatias licha* and *Squalus acanthias*) were collected as by-catch fishes during the Hoki survey, NIWA scientific cruise from January to February 2018 aboard the RV Tangaroa.

2.2. Spectroscopic analysis: sample preparation

Liver oil was extracted based on Folch's protocol (lipid extraction) (Folch et al., 1957). Preliminary, 1 g of the anterior part and 1 g of the posterior part of the liver were collected from complete livers (different lobes included) maintained at −80 °C. Both parts of the liver were then mixed together and this process was repeated in triplicate on the liver of each individual. Folch's protocol was then applied to each sample

individually. Homogenates were centrifuged in chloroform/methanol (2:1) solution and the supernatant containing the lipids was then extracted. Methanol contamination was removed in a saline phase and at the end of the process, samples were left overnight in an incubator at 40 °C to allow the total evaporation of the chloroform. Finally, the total volume of the lipids extracted from the 2 g-liver sample was measured to approximate the percentage of lipids present in the whole liver as percentage of volume by weight of tissue. 500 µl of the lipid extract was then transferred in a closed glass cylinder and maintained at 4 °C until analysis.

2.3. FT-MIR analysis

IR absorption spectra were acquired using a FT-MIR (Fourier Transform Mid Infrared) spectrometer VERTEX 70 (Bruker, Germany) connected to a diamond attenuated total reflectance accessory (diamond ATR) on which are presented the oils. Absorbance spectra are obtained using OPUS 7.2 software (Bruker Optics Inc., Billerica, MA, USA) in a range of 4000-600 cm^{-1} and 64 co-added scans were acquired with a spectral resolution of 4 cm^{-1}. Three replicates were collected for each sample and spectral backgrounds were acquired between each triplicate with a cleaning step between each analysis. Air was considered as a background.

2.4. FT-Raman analysis

Fourier transform Raman (FT-Raman) spectra were acquired using a FTIR (Fourier Transform Infrared) spectrometer VERTEX 70 (Bruker, Germany) connected to a module Ram II. Raman scattering was generated using a 1064 nm diode laser. A laser power of 600 mW was used. FT-Raman spectra were measured in the range of 3600-200 cm^{-1} with a spectral resolution of 4 cm^{-1} (128 scans were co-added per spectrum), using OPUS 7.2 software (Bruker Optics Inc., Billerica, MA, USA). Liquid samples of liver lipid extracts (500 µl) were presented in glass tubes and analyzed in duplicate.

2.5. Spectral pre-processing and multivariate analysis

2.5.1. Qualitative analysis

Unscrambler v10.2 software from CAMO (Computer Aided Modelling, Trondheim, Norway) was used to perform spectral pre-processing and multivariate analysis. To be able to identify each absorption band of the mean spectrum of each species, the spectra of several standards were first analyzed (Squalene, Triolein, Tripalmitin, Dipalmitin and Chloroform, all sourced from Sigma-Aldrich, Belgium). Following spectral analyses and absorption bands identifications, the peaks relevant for the different lipid classes of interest (squalene, TAG and DAGE) were selected for multivariate analysis. In this regard, FT-Raman spectra were used to generate a PCA by selecting the ranges of the spectra containing the peaks associated to squalene (1667 cm^{-1}, from 1765 to 1628 cm^{-1}; 1382 and 1282 cm^{-1}, from 1404 to 1233 cm^{-1}) (Baeten et al., 2001), allowing to separate the samples based on this component. FT-MIR spectra were used to generate a PCA based on the ranges of the spectra associated with peaks corresponding to DAGE and TAG (3380 cm^{-1}, 1740 cm^{-1} and 1118 cm^{-1}).

2.5.2. Quantitative analysis

Squalene concentration was measured using partial least square regression (PLS-R), as usually used in the literature (Tewari and Irudayaraj, 2004; Cozzolino et al., 2005; Meissl et al., 2007; Hall et al., 2016). For this purpose, six different squalene concentrations were made by serial dilution (100%, 50%, 25%, 12.5%, 6.25%, 3.125%) and used to allow the calibration of the PLS-R model. Several spectral pre-processing were tested (no pre-processing, standard normal variate and first derivative) and their performance were compared by measuring the root mean standard error cross validation (RMSECV) and the determination coefficient (R^2) of each model. Based on these data, PLS-R without any pre-treatment was selected among the three models.

TAG and DAGE quantification was uncertain because peaks used to describe these lipid classes display a large, unspecific range (wide band at 3300 cm^{-1}), were localized in the fingerprint region (many information; 1118 cm^{-1}) or were common to both classes (TAG and DAGE contain C=O groups; 1744 cm^{-1}).

2.6. Red aerobic muscle distribution and quantification

The protocol used for red aerobic muscles quantification and distribution is identical to the one from Bernal et al., 2003, to allow the comparison of our results with the literature. Ten different species (*E. spinax*, *E. molleri*, *E. granulosus*, *I. brasiliensis*, *D. licha*, *D. calcea*, *C. squamosus*, *C. owstonii*, *S. plukenti* and *S. acanthias*) were analyzed with 3 to 4 specimens by species. We started to cut the transverse sections from 25% of the fork length (FL) because the quantity of red aerobic muscles was insignificant at the anterior part of the body. Red aerobic muscles are also found in the pectoral fins but do not generate thrust and thus were not considered in this study. Each transverse section measured 5% of the FL, until the caudal peduncle (85–95% FL) was photographed on their anterior and posterior sides.

Pictures were analyzed with ImageJ2© software (Rasband, W.S., ImageJ, U. S. National Institutes of Health, Bethesda, Maryland, USA, https://imagej.nih.gov/ij/, 1997–2018) to measure the red aerobic muscles area on the anterior and posterior sides of the section. The longitudinal red aerobic muscle distribution was obtained by transforming the area (cm^2) measured at 50% of the FL as a reference value of 1. Other positions along the body are thus calculated accordingly to this reference point. The red aerobic muscle volume for each cross section is the product of the section thickness and its red aerobic muscles area (mean between the anterior and the posterior area of the transverse section). The red aerobic muscle mass was measured as the product of red aerobic muscle volume and red aerobic muscles density (literature value confirmed on our shark samples: 1.05 $g.cm^{-3}$). The quantification of the total red aerobic muscle mass (TRMM) was determined by the sum of each section mass value. Finally, this TRMM is compared with the total body mass to quantify the red aerobic muscles proportion. This methodology was validated by removing and weighing the red aerobic muscles of four *I. brasiliensis* previously analyzed.

2.7. Buoyancy index

Due to the lack of an existing 'model of buoyancy', we used a proxy to evaluate the contribution of the shark's liver to the hydrostatic force (Treberg and Speers-Roesch, 2016). This proxy relies on (1) the hepatosomatic index (HIS, % of liver mass according to the total body mass); (2) the oil content of the liver (OC, % of lipid oil by wet mass); and (3) the liver lipid density (LLD, corresponding to the weighting of each lipid class proportion and their respective density).

$$HSI\ (\%) = \left(\frac{Liver\ mass\ (g)}{Total\ body\ mass\ (g)}\right) \times 100 \quad (1)$$

$$OC\ (\%) = \left(\frac{Total\ lipid\ volume\ (ml)}{liver\ mass\ (g)}\right) \times 100 \quad (2)$$

$$LLD = (0.92 \times \%TAG) + (0.89 \times \%DAGE) + (0.86 \times \%HC) + (0.86 \times \%WE) \quad (3)$$

By combining the HSI and the OC we calculated the liver lipid ($g.kg^{-1}$ of shark) and finally inferred the hydrostatic force provided by the liver (Liver Hydrostatic Force -LHF) of the shark by the following Eq. (4), as previously mentioned by Treberg and Speers-Roesch, 2016:

$$LHF = \left(\frac{liver\ lipid\ (g.\ kg^{-1}\ of\ shark)}{LLD\ (g.\ ml^{-1})}\right) \times (sea\ water\ density\ (g.\ ml^{-1}) - LLD\ (g.\ ml^{-1}))\quad (4)$$

where sea water density is 1.025 g.ml^{-1}.

Based on this proxy, a shark with a large liver that is rich in oil of low density lipids will display a high LHF value from its liver (deep-sea squaloid sharks were evaluated with a LHF value around 35 g per kg of shark by Treberg and Speers-Roesch, 2016). In contrast, a shark with a small liver with low oil content and rich in high density lipids will show a low LHF value (shallow-water squaloid sharks were evaluated with a LHF value around 7 g per kg of shark by Treberg and Speers-Roesch, 2016. The hydrostatic force contribution of shark livers was tested and validated using overall tissue density and liver density of sharks from the literature (Treberg and Speers-Roesch, 2016; Gleiss et al., 2017). Strong linear relations were obtained with $r^2 = 0.84$ between the LHF and the overall tissue density (Linear regression, F1, 10 = 2912.84, $P < .001$) and $r^2 = 0.80$ between the LHF and the liver density (Linear regression, F1, 10 = 2912.84, $P < .001$) (additional information and data available in supplementary data 1 and 2). For four species (*E. spinax*, *E. molleri*, *I. brasiliensis* and *G. melastomus*) the quantitative analysis of DAGE and TAG was not possible. Only semi-quantitative values were obtained, with a prevalence of one or the other lipid class. Therefore, every analysis was based on with the minimum and maximum concentration of each lipid class and graph representations were done using a 50/50 proportion of each class. The LHF values calculated from our results and literature data (*E. granulosus, D. licha, C. owstonii, C. squamosus, D. calcea, S. acanthias, P. glauca, L. ditropis* and *Alopidae sp.*) were related to the median depth of occurrence corresponding to the mean between the maximal and the minimal recorded depth for each species (Ebert et al., 2013).

2.8. Statistical analyses

All univariate statistical analyses (univariate parametric test) were performed with JMP pro 14 (JMP®, Version < 14 > . SAS Institute Inc., Cary, NC, 1989–2007). The normality and the homoscedasticity were confirmed for each parametric test.

3. Results

All data collected from our research and literatures are summarized in the Table 1, detail data for the liver hydrostatic force calculation are in Supplementary data 2.

3.1. Lipid composition: spectroscopic analyses

The mean spectra obtained by FT-Raman and FT-MIR spectroscopy are presented on Fig. 1. Letters allow the differentiation between the spectral regions of interest based on their molecular vibrations. Each absorption band was identified based on its molecular vibrations and the preliminary analyses of the spectra of the standards (Table 2).

The complete analysis of the spectra of the standards and the samples allowed the identification of the spectral region of interest (containing the three relevant lipid classes: squalene, TAG and DAGE) in FT-Raman and FT-MIR data. In this way, on one hand, FT-Raman spectroscopy allowed a better resolution of the peaks associated to squalene (1667 cm^{-1}, corresponding to the additive intensity of the 6 double bonds C=C; 1382 cm^{-1}, corresponding to several molecular vibrations such as stretching of C-C; 1282 cm^{-1}, corresponding to bending vibrations of the methyl or methylene group) (Baeten et al., 2001). On the other hand, FT-MIR spectroscopy allowed the distinction of the peaks associated to the DAGE (wide band around 3300 cm^{-1} and peak at 1118 cm^{-1} corresponding to O–H and C–O stretching

Table 1
Summary of data collected from this study and the literature on the 14 species of sharks; median depth occurrence (MDO) corresponds to the mean between the maximum and the minimum depth where shark was observed (m), Hepatosomatic index (HSI % ± SD), Oil content correspond to the percentage of lipid g wet mass^{-1} (OC % ± SD), Percentage composition of main lipid classes in shark liver: TAG = Triacylglyceride, DAGE = Diacylglyceride, HC = Hydrocarbon, mainly squalene (Tsujimoto, 1916) and WE = Wax Ester (% ± SD), g of hydrostatic force per kg of shark (LHF), Red aerobic muscle position (RML) where HLP = Highly Lateral and Posterior and PL = Posterior and Lateral, proportion of red aerobic muscles (RM % ± SD), Ref. corresponds to the literature sources: [1]Wetherbee and Nichols, 2000; [2]Pethybridge et al., 2010; [3]Bernal et al., 2003; [4]Jayasinghe et al., 2003a; [5]Jayasinghe et al., 2003b; [6]Sepulveda et al., 2005; [7]Treberg and Speers-Roesch, 2016; [8]Mull et al., 2013.

Order/species	Habitat	MDO (m)	HSI (%)	OC (%)	TAG (%)	DAGE (%)	HC (%)	WE (%)	LHF (g.kg^{-1} of shark)	RML	%RM	Ref.
Squaliformes												
Isistius brasiliensis	Deep	1793	18.8 ± 0.6	71.5 ± 4.9	< 29	> 29	41.9 ± 1.6	< 1	20.8	HPL	1.14	Present study
Dalatias licha	Deep	918	20.9 ± 5.2	79 ± 9	2 ± 2	18 ± 13	79 ± 13	< 1	30.1	PL	0.84 ± 0.30	Present study,[1,2]
Etmopterus spinax	Deep	1035	20.2 ± 0.9	69.7 ± 1.9	< 31	> 31	36.9 ± 1.8	< 1	21.3	PL	1.57	Present study
Etmopterus granulosus	Deep	860	18.7 ± 2.7	72 ± 7	9 ± 7	35 ± 11	55 ± 12	< 1	22.8	PL	1.73 ± 0.36	Present study,[1,2]
Etmopterus molleri	Deep	447	5.9 ± 0.5	51.2 ± 2.4	< 50	> 50	< 1	< 1	3.8	PL	2.89 ± 0.67	Present study
Centroscymnus owstonii	Deep	805	20.1 ± 0.2	65 ± 5	22 ± 7	23 ± 8	54 ± 13	< 1	21.1	PL	2.47 ± 0.21	Present study,[1,2]
Deania calcea	Deep	770	19.3 ± 1.3	81 ± 6	9 ± 5	24 ± 6	67 ± 8	< 1	27.1	PL	1.21 ± 0.14	Present study,[1,2]
Centrophorus squamosus	Deep	1315	21.4	83 ± 3	18 ± 5	11 ± 6	70 ± 6	< 1	30.2	PL	1.84 ± 0.08	Present study,[1,2]
Squalus acanthias	Shallow	300	8.7 ± 2.5	41.3 ± 4.6	74.7 ± 4.3	15.7 ± 1.2	< 1	< 1	3.9	PL	2.54 ± 0.52	Present study,[1,2]
Carcharhiniformes												
Galeus melastomus	Shallow	528	10 ± 0.6	69.9 ± 1.9	> 50	< 50	< 1	< 1	8.9	/	/	Present study
Prionace glauca	Shallow	175	6.7 ± 1.1	49.9 ± 0.6	72.3 ± 1.1	2.7 ± 0.4	11 ± 0.4	< 1	3.9	PL	2.65 ± 0.56	[3,4]
Lamniformes												
Lamna ditropis	Shallow	188	7.3 ± 0.9	48.3 ± 10	80.4 ± 4.6	2.8 ± 1.4	4.4 ± 1.8	< 1	3.9	AC	2.09	[3,5]
Alopias superciliosus	Shallow	200	5.4 ± 1.2	36 ± 0.5	80.7 ± 1.4	1.1 ± 0.3	5 ± 0.5	< 1	2.2	AC	2.31 ± 0.21	[4,6]
Carcharodon carcharias	Shallow	650	12.7 ± 3.1	63 ± 15.5	93.3	< 1	< 1	< 1	7.9	AC	2.06 ± 0.12	[3,7,8]

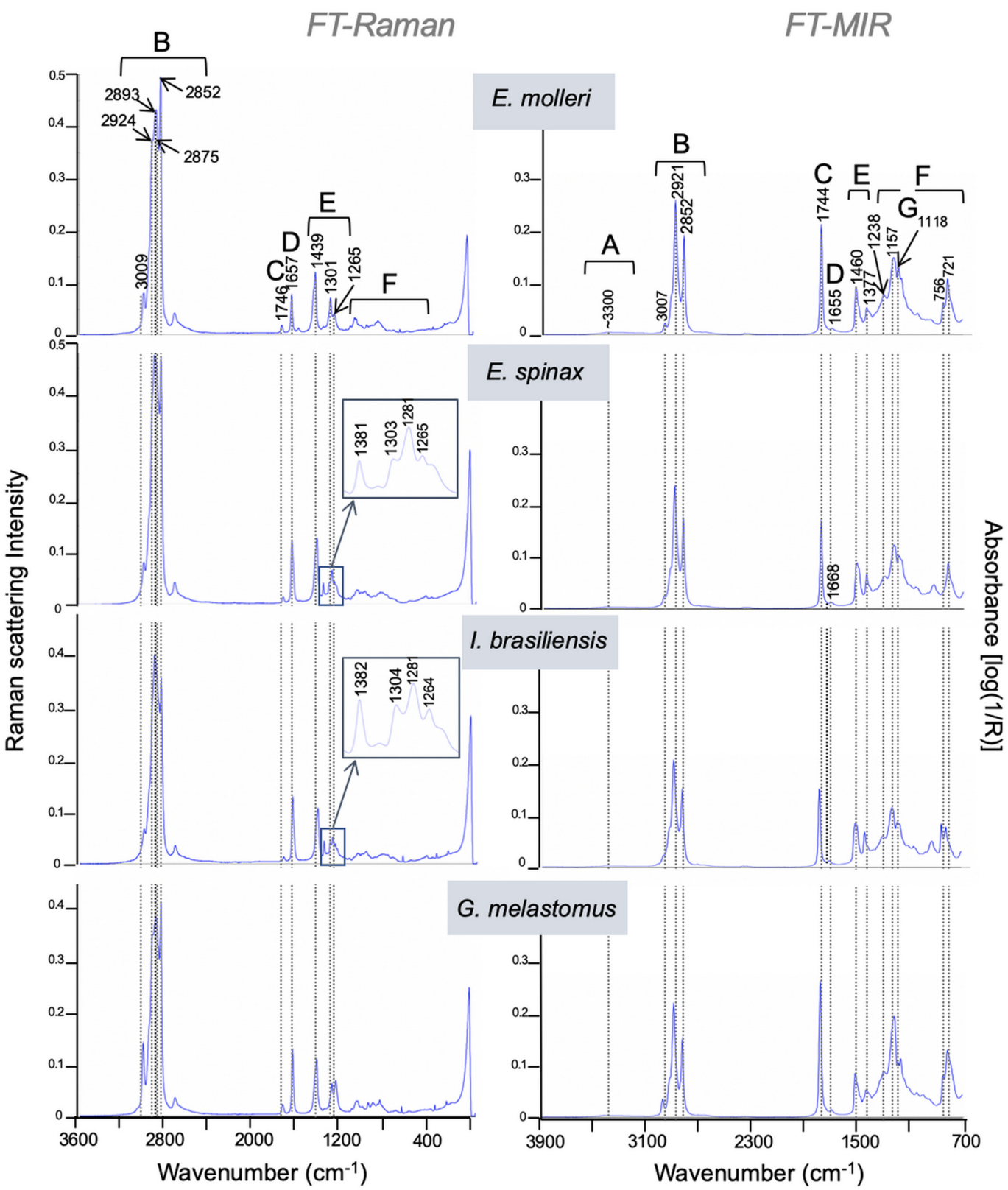

Fig. 1. Mean spectra of the four studied species obtained with FT-Raman and FT-MIR. The letters (A, B, C, D, E, F, G) separate the spectral region of interest.

vibrations, respectively) and to the TAG (1744 cm^{-1}, corresponding to C═O stretching vibrations) (Vermeulen et al., 2015).

3.1.1. Qualitative analyses

PCA models have been developed on FT-Raman and FT-MIR spectral data of studied species without application of any chemometric pretreatment. In FT-Raman, a PCA realized on the spectral ranges containing the peaks specific to squalene allowed a reliable differentiation between the squalene content of the several studied species (Fig. 2 AB). The analysis of these results shows that the species that are richer in

Table 2
FT-Raman and FT-MIR absorption bands identification of the mean spectra of the four studied species, based on bands identification of the standards (O'Connor et al., 1955; Baeten, 1998; Socrates, 2001; Chun et al., 2013; Czamara et al., 2014; Laachari et al., 2015; Hall et al., 2016).

Region	Wavenumber (cm^{-1})								Vibration
	Em		Es		Ib		Gm		
	Raman	MIR	Raman	MIR	Raman	MIR	Raman	MIR	
A		~3300		~3300		~3300		~3300	Stretching O—H
B	3009	3007	3009	3003	3009	3003	3014	3011	Stretching C—H
B	2924	2921	2927	2921		2921	2924	2921	Symetrical Stretching CH3/ Asymetrical CH2
B			2913		2913				Symetrical Stretching CH3/ Asymetrical CH2
B	2893		2893		2893		2893		Asymetrical Stretching CH3
B	2875		2875		2875		2875		Asymetrical Stretching CH2
B	2852	2852	2852	2852	2852	2852	2852	2852	Symetrical Stretching CH2
C	1746	1744	1746	1744	1746	1744	1746	1744	Stretching C=O
D			1667	1668	1667	1668			Stretching *trans* C=C
D	1657	1655					1657	1655	Stretching *cis* C=C
E	1451	1460	1451	1456	1451	1452	1451	1430	Bending CH2 (Scissoring)
E	1439		1436		1439		1439		Bending CH2 (Scissoring)
E			1382		1382				Bending CH_3 symetrical/CH_2 (Wagging)/C—H (Wagging)/ stretching C—C
E		1377		1377		1377		1377	Bending CH3 symetrical/CH2 (Wagging)
E			1329		1329				Bending CH2 (Wagging)
E	1301		1303		1303		1301		Bending CH2 (Twisting)
E			1282		1282				Bending CH_3 symmetrical/CH_2 (Twisting)
E	1265		1265		1265		1265		Bending=CH
F		1238, 1157		1232, 1157		1234, 1157		1230, 1157	Stretching C—C
G		1118		1118		1118		1118	Stretching C—O
F	1079, etc.	1097, etc.	1079, etc.	1097, etc.	1079, etc.	1097, etc.	1079, etc.	1097, etc.	Stretching C—C
F				832		832			Bending C—C (Rocking)

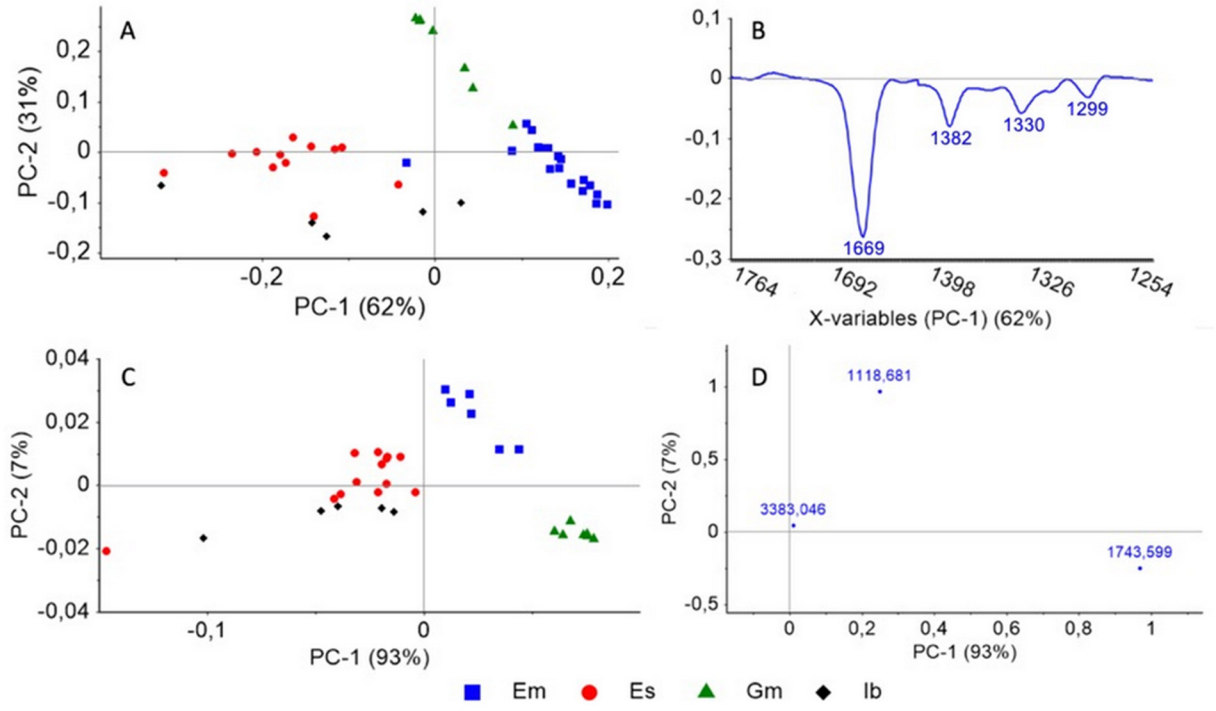

Fig. 2. Scores (PCA) and loadings obtained (A,B) by selecting the FT-Raman spectral ranges containing the peaks of squalene (from 1765.16 to 1628.2 cm^{-1} and 1404.5 to 1233.8 cm^{-1}); (C,D) by selecting the FT-MIR spectral peaks (3383.5, 1743.8 and 1118.8 cm^{-1}). Each dot represents one individual. Em, *Etmopterus molleri*; Es, *Etmopterus spinax*; Gm, *Galeus melastomus*; Ib, *Isistius brasiliensis*.

squalene are *Isistius brasiliensis* and *Etmopterus spinax*. More specifically, the direct observation of the peaks associated to squalene (1669, 1382 and 1282 cm^{-1}) pre-treated as first and second derivative showed that these two former species are the only out of the four studied species containing squalene. The results obtained in FT-MIR, by selecting the three peaks characterizing DAGEs and TAGs (Fig. 2 CD) show that *Galeus melastomus* contains more TAGs (1743 cm^{-1}, C=O stretching vibrations) and that *Etmopterus molleri* contains more DAGEs (1118 cm^{-1}, O—H stretching vibrations that is absent in TAGs and in the main fatty acids found in DAGE and TAGs in animal oils (O'Connor et al., 1955; Sargent et al., 1972; Deprez et al., 1990; Bakes and Nichols, 1995; Davidson and Cliff, 2002; Pethybridge et al., 2010; Czamara

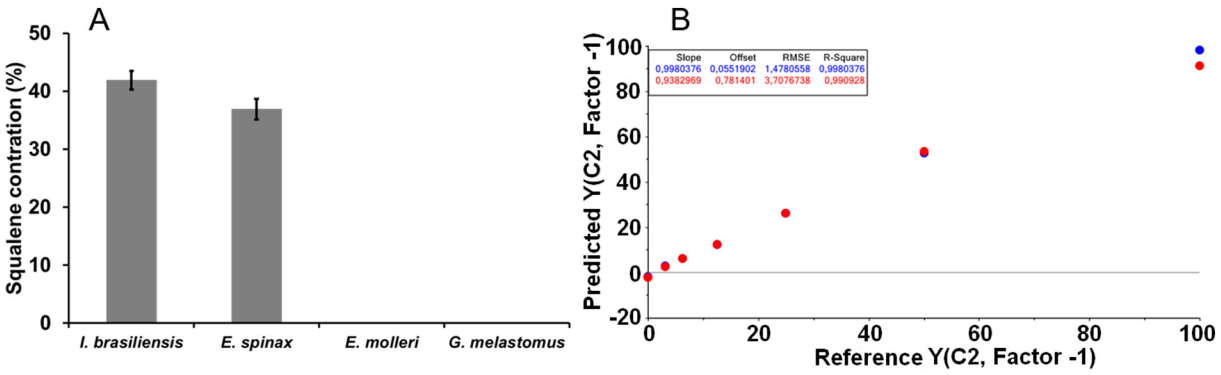

Fig. 3. (A) Squalene concentration of the liver oil lipid fraction of each shark species studied. Quantification was possible through PLS-R; (B) PLS regression on spectral ranges containing the peaks of squalene (1667 cm^{-1}: from 1692 to 1638 cm^{-1}; 1382 cm^{-1}: from 1392 to 1368 cm^{-1}; 1282 cm^{-1}: from 1291 to 1272 cm^{-1}) from six different squalene concentration samples (100%, 50%, 25%, 12.5%, 6.25%, 3.125%). In blue, the calibration dots; in red, the cross-validation dots. RMSE, Root Mean Square Error.

et al., 2014).

3.1.2. Quantitative analyses

PLS-R was based on FT-Raman spectra of six different squalene samples with known concentrations. The model was then applied on studied species to quantify the squalene concentration in the liver oil samples (Fig. 3B). No pre-treatment has been applied and only spectral regions characteristic of squalene were considered (1692-1638 cm^{-1} (peak at 1667 cm^{-1}), 1392-1368 cm^{-1} (peak at 1382 cm^{-1}) and 1291-1272 cm^{-1} (peak at 1282 cm^{-1}). Developed regression model showed a very high coefficient of determination ($R^2 = 0.99$) and a root mean square error of cross-validation RMSECV equal to 2.3. Results showed that *Isistius brasiliensis* contains ~41.9% of squalene in its liver oil, followed by *Etmopterus spinax* with 36.9% then by both *Etmopterus molleri* and *Galeus melastomus* which showed values close to 0% (Fig. 3A).

3.2. Contribution of the liver hydrostatic force according to the median depth of occurrence (MDO)

Statistical analysis of the contribution of the liver to the hydrostatic force reveals a strong difference between deep-sea sharks (e.g. living mostly under 200 m depth) and shallow-water sharks (e.g. living mostly above 200 m depth). Deep-sea sharks have a higher mean value (22.16 ± 2.97 g per kg of shark) than mean value of shallow-water counterparts (5.12 ± 1.09 g per kg of shark) (Student's *t*-test, t13, $P < .001$) (Fig. 4A). One deep-sea species, *E. molleri*, is clearly an outlier with a lower value than other deep-sea species (Fig. 4A). The linear regression between the hydrostatic force provided by the liver and the MDO is significant (Linear regression, $r^2 = 0.59$, F1, 13 = 1524.53, $P < .05$) (Fig. 4B). The following equation, LHF = −2.09 + (0.02 x MDO), shows a linear increase with depth.

3.3. Red aerobic muscle distribution and red aerobic muscle mass

All sharks display a posterior lateral (PL) distribution of their red aerobic muscles. *E. molleri*, *E. granulosus*, *C. squamosus*, *D. calcea*, *D. licha*, *C. owstonii* and *S. acanthias* display a similar red aerobic muscle distribution pattern, with contents increasing along the fork length to reach their maximal values at 55%, 65%, 70%, 65%, 60%, 70% and 65%, respectively (Fig. 5 A-G for deep-sea species and H for shallow-water one). For all these species, the red aerobic muscle proportion rapidly declines to zero at fork length values between 85% and 90%. While *Isistius brasiliensis* displays a red aerobic muscle distribution slightly different, red aerobic muscle proportions reach a maximum around 85% of the fork length with a small proportion remaining at the end of the fork. We therefore characterized this distribution as highly posterior lateral (HPL). Mean values of red aerobic muscles proportions are summarized in Table 2; mean value analysis shows a significant difference between deep-sea sharks displaying fewer red aerobic muscles (1.71 ± 0.69% RM) than their shallow-water counterparts (2.4 ± 0.25% RM) (Student's *t*-test, t10, $P < .001$). Finally, two of the eight deep-sea shark species, *E. molleri* and *C. owstonii*, show a red aerobic muscle mass that is more characteristic of shallow-water species (2.64 ± 0.67% RM and 2.47 ± 0.21% RM, respectively).

3.4. Contribution of the liver hydrostatic force according to the red aerobic muscle proportion

The linear regression between the hydrostatic force of the liver and the red aerobic muscle proportion is significant (Linear regression, $r^2 = 0.59$, F1, 13 = 4.79, $P < .05$). The following equation, LHF = 2.62 - (0.04 x red aerobic muscle proportion), reveals a linear decrease with the red aerobic muscle proportion (Fig. 6).

4. Discussion

Our study highlights the benefits of spectroscopic techniques for shark liver oil analysis, as a rapid, non-destructive, reliable and less laborious technique than conventional ones (Abbas et al., 2009; McGoverin et al., 2009; Chiu et al., 2017; Tiryaki and Ayvaz, 2017). Previous studies on shark liver oil focused on squalene determination (Chun et al., 2013; Hall et al., 2016) but ours allows to complete the previous spectral analysis by the characterization of the absorption bands specific to squalene (FT-Raman), DAGEs and TAGs (FT-MIR), also highlighting the complementarity of these two techniques. However, quantification was only possible for squalene (PLS-R) while FT-MIR spectroscopy only allowed a semi-quantitative determination of TAGs and DAGEs, emphasizing the need to identify other specific absorption bands for these lipid classes through further spectral analyses or through the use of traditional lipid approaches in parallel.

Previous studies have suggested that sharks may be either negatively, neutrally (Corner et al., 1969; Wetherbee and Nichols, 2000) or even positively (Nakamura et al., 2015) buoyant. The buoyancy capability of sharks seems to be one of the major constrain explaining their actual distribution. For example, (i) fewer cartilaginous species are observed in fresh waters due to a 2- to 3-folds increase in negative buoyancy in these environments (Gleiss et al., 2015); (ii) fewer shark species are found in the deep-sea cold environment because of the metabolic costs associated with large livers (Priede et al., 2006; Treberg and Speers-Roesch, 2016). Due to the cold and oligotrophic environment of the deep sea, shark metabolism is reduced, as observed for most species thriving in this environment (Treberg et al., 2003; Condon et al., 2012; Treberg and Speers-Roesch, 2016). Their swimming capabilities

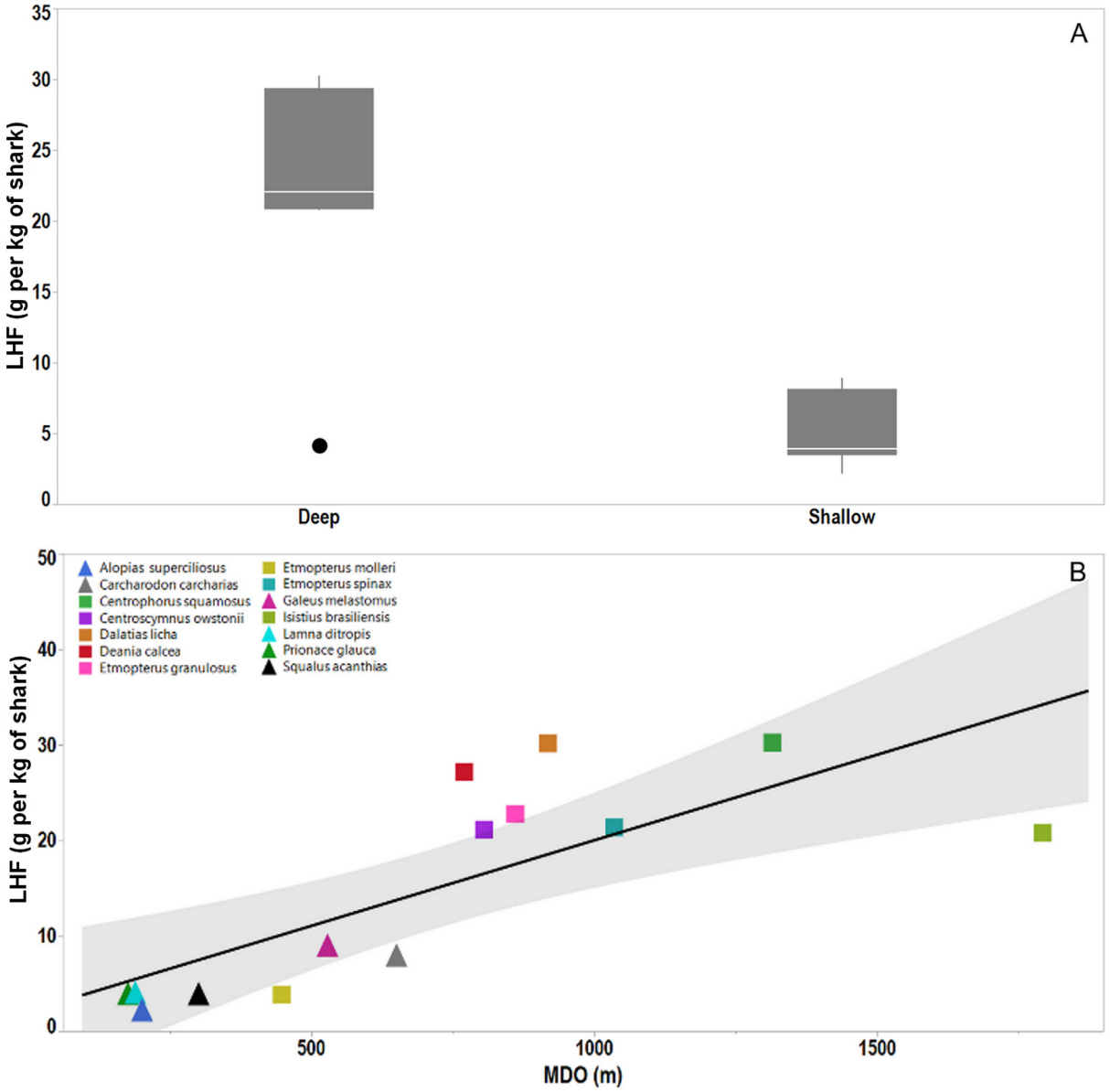

Fig. 4. (A) Boxplot representation of the liver hydrostatic force (LHF – g/kg of shark) according to their habitat; "Deep" corresponds to deep-sea sharks (e.g. living mainly under 200 m depth), "Surface" correspond to shallow-water sharks (e.g. living mainly above 200 m depth); (B) Linear regression of the liver hydrostatic force (LHF – g kg-1 of shark) according to the median depth of occurrence (MDO) of 14 different shark species (cfrs. Graph legend), "MDO" corresponds to the mean between the maximal and the minimal depth recorded for each shark species and is expressed in meters; ▲corresponds to shallow-water sharks and ■ corresponds to deep-sea sharks. Dark grey region corresponds to the confidence region (0.95) for the fitted line.

are altered by this constrain and buoyancy close to the neutrality may act as a way to reduce the energetic cost of lowered swimming capabilities. Indeed, negative buoyancy was shown to be favorable for fast moving species (Alexander, 1990; Gleiss et al., 2017) whereas less negative buoyancy becomes increasingly efficient as routine swimming speeds declines (Gleiss et al., 2017). Our study provides data in favor of this approach, through the characterization of the liver oil composition of three new species of deep-sea sharks and the comparison with a shallow-water counterpart. More specifically, our results showed that *G. melastomus* (shallow-water species) displays a low HSI, a liver rich in oil content that has no squalene and is more characterized by TAGs, the lipid class providing a low hydrostatic force. In contrary, deep-sea species (*I. brasiliensis* and *E. spinax*) display a high HSI, with livers rich in oil containing squalene as a predominant lipid class (providing more hydrostatic force). However, *E. molleri* shows unusual liver features for a deep-sea species: low HSI and low liver oil content mainly composed of DAGEs, suggesting this shark to have buoyancy characteristics closer to shallow-water species than deep-sea ones. Some studies have shown that several deep-sea sharks do not have squalene (Pethybridge et al., 2010) and tend to accumulate DAGEs in higher concentrations as compensation (Treberg and Speers-Roesch, 2016). However, even if *E. molleri* liver was composed of a 100% of DAGEs, it would not be sufficient to get a similar LHF value than deep-sea sharks, according to the equation.

In our study, the red aerobic muscle distributions of most deep-sea shark species were similar with the ones found in most shallow-water shark species (Bernal et al., 2003). The red aerobic muscles were mainly located in the half posterior of the body, in lateral position just below the skin. These red aerobic muscle fibers were connected with the skin as well as white muscle fibers located just underneath (Kryvi and Eide, 1977). Red fibers are powered by aerobic metabolism during cruise swimming mode (i.e. usual fish swimming mode) (Treberg et al., 2003).

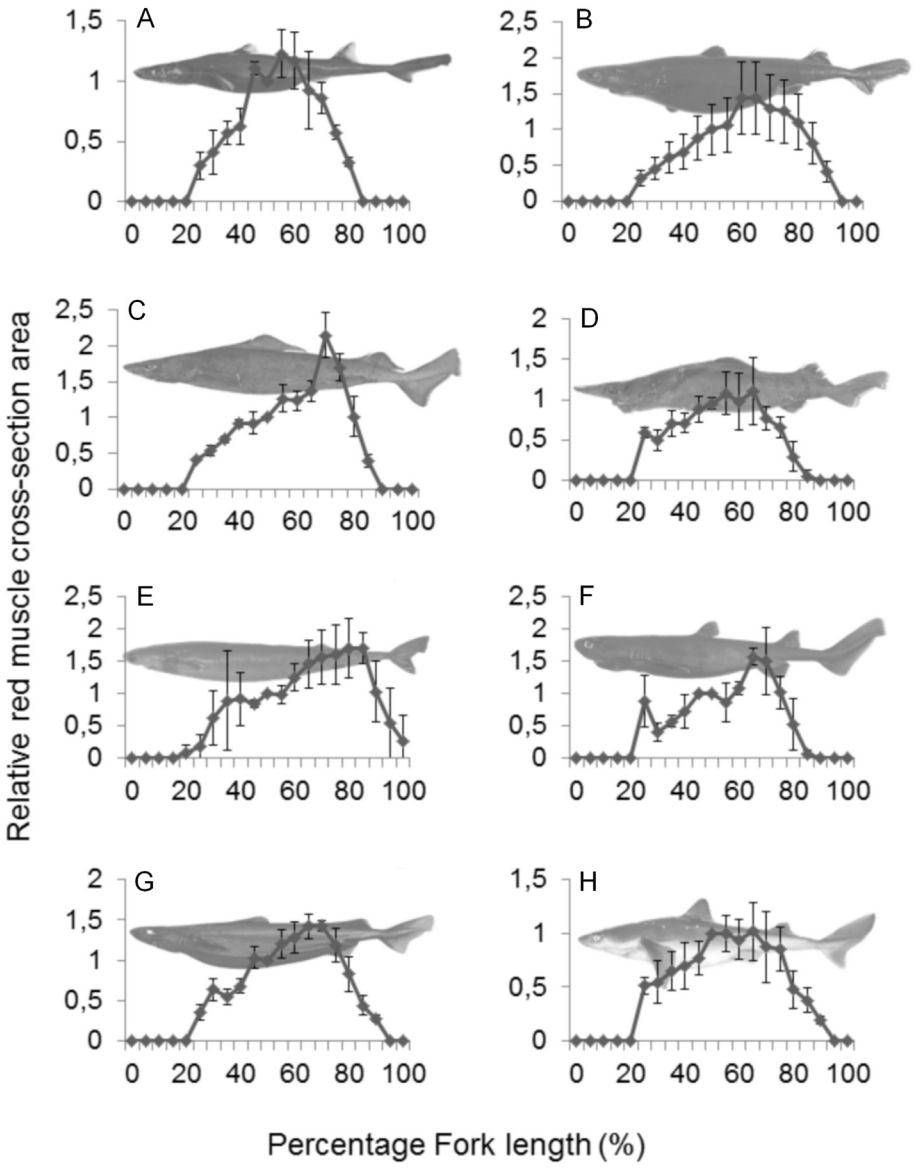

Fig. 5. Red muscle (RM) distribution pattern in seven deep-sea shark species (A-G) and on shallow-water shark species (H). All sharks have posterior and lateral distribution of their RM (PA): (A) *Etmopterus molleri*; (B) *Etmopterus granulosus*; (C) *Centrophorus squamosus*; (D) *Deania calcea*; (E) *Isistius brasiliensis*; (F) *Dalatias licha*; (G) *Centroscymnus owstonii*; (H) *Squalus acanthias*. The relative amounts of RM in the different positions along the body are expressed as a proportion of the RM cross-sectional area equal to 1 at 50% fork length. Values are means ± S.E.M. Shark illustrations are modified from fishes of Australia.

Only *I. brasiliensis* displayed a slightly different red aerobic muscle distribution with most of the red aerobic muscles located close to the caudal fin. This result could explain the thunniform swimming mode observed for this species. Indeed, red aerobic muscle concentration next to the caudal region gathers all red muscles contraction around this location but mechanistical studies should be performed to understand better this particularity and its use. Thanks to the red aerobic muscles distribution, we were able to calculate the red aerobic muscle proportion corresponding to the red aerobic muscle mass divided by the total body mass. Results showed that deep-sea sharks have less red aerobic muscles than their shallow-water counterparts with the exception of *E. molleri*, which exhibited a red aerobic muscle proportion similar to shallow-water sharks.

Finally, it has been proposed that sharks with neutral buoyancy would need less red aerobic muscle fibers than those with negative buoyancy as it is an advantage for slow swimming mode (Bone, 1966). Our results show a strong relationship between the liver hydrostatic force and the red aerobic muscle proportions which supports Bone's hypothesis. Indeed, as deep-sea sharks have a lower metabolism, their tail beat is thus slowed and their swimming speed reduced. As fewer works are performed in the caudal region, less red aerobic fibers are needed. To compensate this lowered thrust, sharks require higher hydrostatic force.

While numerous studies have investigated the buoyancy of marine organisms through density measurements, modelling of some features involving the buoyancy, our study use the liver to examine a part of shark buoyancy and its relation with the muscular composition. To reflect correctly the buoyancy of shark, we need to incorporate all parameters which can have impacts on it: temperature, osmolytes composition, other tissue densities, etc. However, the main role of liver in the hydrostatic buoyancy and the change of its features through species make it a good proxy for buoyancy estimation.

5. Conclusion

The FT-Raman and FT-MIR spectroscopy have allowed the

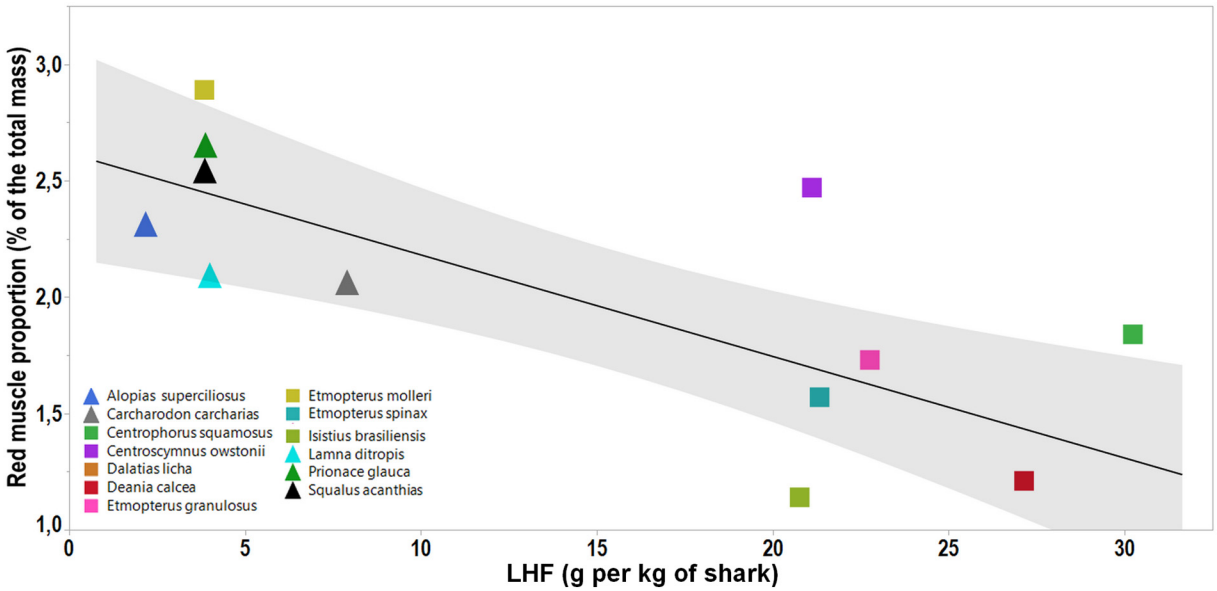

Fig. 6. Linear regression of the liver hydrostatic force (LHF – g kg-1 of shark) according to the red muscle proportion of 13 different shark species (see graph legend). ▲corresponds to shallow-water sharks and ■ corresponds to deep-sea sharks. Dark grey region represents the confidence region (0.95) for the fitted line.

identification of the different lipid classes found in shark liver oil and to quantify its squalene composition. Further spectral analyses should allow to quantify the two main other lipid classes (DAGEs and TAGs). Our results combined with data from the literature suggest that most deep-sea shark species studied have livers that provide higher hydrostatic force than shallow-water sharks, according to the LHF equation. They also highlight an increase of the buoyancy provided by the liver as a function of the median depth of occurrence of the shark. Finally, the 1966 Bone's hypothesis is supported by showing a relation between the red aerobic muscle proportion and the buoyancy provided by the liver. However, a complete modelling of the buoyancy of sharks would be essential for further research on this topic.

Acknowledgement

We really thank Quentin Arnould from CRA-W for the time he spent to explain and help us about the FT-Raman and FT-MIR spectroscopy. We also thank Laurent Duchatelet from the marine biology laboratory of UCL for the help provided during the *Etmopterus spinax, Etmopterus molleri* and *Galeus melastomus* liver sampling. Finally, we thank Emma Jones from NIWA Auckland to collect and deliver the deep-sea sharks from the Hoki Survey to the physiological lab of NIWA in Wellington, New Zealand.

Author contribution

N.P., J.M. & M.G. collected data and contributed equally to the data analyses and the article preparation. O.A. and *V*.B. provided all the technical spectroscopy support and helped during the spectral data analyses. All authors reviewed the final version and agree to final article submission.

Funding

This work was supported by a grant from the Fonds de la Recherche Scientifique (FRS-FNRS, Belgium) to N.P. & J.M. and by the Centre Wallon de recherches agronomiques (CRA−W) to V.B. & O.A.

Ethical issues

Etmopterus spinax, *Galeus melastomus* were collected in Norway under the "experimental fish care permit" number 12/14048. *Etmopterus molleri* were collected and handled according to Churaumi aquarium husbandry and veterinary rules for fish experimentations. All sharks were euthanized by a knock on the chondrocranium followed by an incision at the level of the spinal cord, following the local rules for experimental fish care and the European regulation for research animal handling. *Isistius brasiliensis* was fished as by-catch specie in La Reunion Island. *Centroscymnus owstonii*, *Centrophorus squamosus*, *Deania calcea*, *Dalatias licha*, *Etmopterus granulosus*, *Squalus acanthias* were collected as by-catch species during the Hoki survey around the Chatham Rise in New Zealand. These species are not in the CITES list.

Appendix A. Supplementary data

Supplementary data to this article can be found online at https://doi.org/10.1016/j.cbpa.2019.06.020.

References

Abbas, O., Pierna, J.F., Codony, R., Von Holst, C., Baeten, V., 2009. Assessment of the discrimination of animal fat by FT-Raman spectroscopy. J. Mol. Struct. 924, 294–300.
Alexander, R.M., 1990. Size, speed and buoyancy adaptations in aquatic animals. Am. Zool. 30 (1), 189–196.
Baeten, V., 1998. Virgin Oil Authentification by Fourier Transform Raman Spectroscopy (PhD. thesis). Université catholique de Louvain-la-Neuve, Belgique & Instituto de la Grasa, Seville, Espagne.
Baeten, V., Dardenne, P., Aparicio, R., 2001. Interpretation of Fourier transform Raman spectra of the unsaponifiable matter in a selection of edible oils. J. Agric. Food Chem. 49, 5098–5107.
Bakes, M.J., Nichols, P.D., 1995. Lipid, fatty acid and squalene composition of liver oil from six species of deep-sea sharks collected in southern Australian waters. Comp. Biochem. Physiol. Part B Biochem. Mol. Biol. 110, 267–275.
Bernal, D., Sepulveda, C., Mathieu-Costello, O., Graham, J.B., 2003. Comparative studies of high performance swimming in sharks. Red aerobic muscle morphometric, vascularization and ultrastructure. J. Exp. Biol. 206 (16), 2831–2843.
Bone, Q., 1966. On the function of the two types of myotomal muscle fibres in elasmobranch fish. J. Mar. Biol. Assoc. 46, 321.
Bone, Q., 1978. Locomotor muscles. Fish. Physiol. 7, 361–424.
Bone, Q., Moore, H., 2008. Biology of Fishes, 2rd ed. Taylor & Francis Group, pp. 478.
Bone, Q., Roberts, B.L., 1969. The density of elasmobranchs. J. Mar. Biol. Assoc. United Kingdom 49, 913.
Chiu, L., Ho, S.H., Shimada, R., Ren, N.Q., Ozawa, T., 2017. Rapid in vivo lipid/carbohydrate quantification of single microalgal cell by Raman spectral imaging to reveal salinity-induced starch-to-lipid shift. Biotechnol. Biofuels 10 (1), 9.
Chun, H.J., Weiss, T.L., Devarenne, T.P., Laane, J., 2013. Vibrational spectra and DFT calculations of squalene. J. Mol. Struct. 1032, 203–206.
Clarke, A., Doherty, N., Devries, A.L., Eastman, J.T., 1984. Lipid content and composition

of three species of Antarctic fish in relation to buoyancy. Polar Biol. 3, 77–83.
Condon, N.E., Friedman, J.R., Drazen, J.C., 2012. Metabolic enzyme activities in shallow- and deep-water chondrichthyans: implications for metabolic and locomotor capacity. Mar. Biol. 159 (8), 1713–1731.
Corner, E.D.S., Denton, E.J., Forster, G.R., 1969. On the buoyancy of some deep-sea sharks. Proc. R. Soc. Lond. B Biol. Sci. 171.
Cozzolino, D., Murray, A.I., Chree, A., Scaife, J.R., 2005. Multivariate determination of free fatty acids and moisture in fish oils by partial least-squares regression and near-infrared spectroscopy. LWT-Food Sci. Technol. 38 (8), 821–828.
Czamara, K., Majzner, K., Pacia, M.Z., Kochan, K., Kaczor, A., Baranska, M., 2014. Raman spectroscopy of lipids: a review. J. Ram. Spectrosc. 46 (1), 4–20.
Davidson, B., Cliff, G., 2002. The liver lipid fatty acid profiles of seven Indian Ocean shark species. Fish Physiol. Biochem. 26, 171–175.
Deprez, P., Volkman, J., Davenport, S., 1990. Squalene content and neutral lipid composition of livers from deep-sea sharks caught in Tasmanian waters. Mar. Freshw. Res. 41, 375.
Ebert, D., Fowler, S., Compagno, L., 2013. Sharks of the world. Wild Nature 73–173.
Folch, J., Lees, M., Sloane-Stanley, G.H., 1957. A simple method for the isolation and purification of total lipids from animal tissues. J. Biol. Chem. 226 (1), 497–509.
Gleiss, A.C., Potvin, J., Keleher, J.J., Whitty, J.M., Morgan, D.L., Goldbogen, J.A., 2015. Mechanical challenges to freshwater residency in sharks and rays. J. Exp. Biol. 218 (7), 1099–1110.
Gleiss, A.C., Potvin, J., Goldbogen, J.A., 2017. Physical trade-offs shape the evolution of buoyancy control in sharks. Proc. R. Soc. B Biol. Sci. 284 (1866), 20171345.
Hall, D.W., Marshall, S.N., Gordon, K.C., Killeen, D.P., 2016. Rapid quantitative determination of squalene in shark liver oils by Raman and IR spectroscopy. Lipids 51, 139–147.
Iosilevskii, G., Papastamatiou, Y.P., 2016. Relations between morphology, buoyancy and energetics of requiem sharks. R. Soc. Open Sci. 3 (10), 160406.
Jayasinghe, C., Gotoh, N., Tokairin, S., Ehara, H., Wada, S., 2003a. Inter species changes of lipid compositions in liver of shallow water sharks from the Indian Ocean. Fish. Sci. 69 (3), 644–653.
Jayasinghe, C., Gotoh, N., Wada, S., 2003b. Variation in lipid classes and fatty acid composition of salmon shark (Lamna ditropis) liver with season and gender. Comp. Biochem. Physiol. B 134 (2), 287–295.
Kryvi, H., Eide, A., 1977. Morphometric and autoradiographic studies on the growth of red and white axial muscle fibres in the shark Etmopterus spinax. Ital. J. Anat. Embryol. 151 (1), 17–28.
Laachari, F., Maâtaoui, H., El Bergadi, F., Boukir, A., Ibnsouda, S.K., 2015. Improvement of a lipolytic activity assay protocol to increase the efficiency of the lipases activity measurement and validation by infrared spectroscopy. Afr. J. Biotechnol. 14.
Malins, D.C., Wekell, J.C., Houle, C.R., 1965. Composition of the diacyl glyceryl ethers and triglycerides of the flesh and liver of the dogfish (*Squalus acanthias*). J. Lip. Res. 6 (1), 100–105.
McGoverin, C.M., Clark, A.S.S., Holroyd, S.E., Gordon, K.C., 2009. Raman spectroscopic prediction of the solid fat content of New Zealand anhydrous milk fat. Anal. Method. 1 (1), 29–38.
Meissl, K., Smidt, E., Schwanninger, M., 2007. Prediction of humic acid content and respiration activity of biogenic waste by means of Fourier transform infrared (FTIR) spectra and partial least squares regression (PLS-R) models. Talanta 72 (2), 791–799.
Mull, C.G., Lyons, K., Blasius, M.E., Winkler, C., O'Sullivan, J., Lowe, C.G., 2013. Evidence of maternal offloading of organic contaminants in white sharks (Carcharodon carcharias). PLoS One 8 (4), e62886.
Nakamura, I., Meyer, C.G., Sato, K., 2015. Unexpected positive buoyancy in Deep Sea sharks, Hexanchus griseus, and Echinorhinus cookei. PLoS One 10.
O'Connor, R.T., Dupré, E.F., Feuge, R.O., 1955. The infrared spectra of mono-, di-, and triglycerides. J. Am. Oil Chem. Soc. 32 (2), 88–93.
Payne, N.L., Iosilevskii, G., Barnett, A., Fischer, C., Graham, R.T., Gleiss, A.C., Watanabe, Y.Y., 2016. Great hammerhead sharks swim on their side to reduce transport costs. Nat. Commun. 7, 12289.
Pethybridge, H., Daley, R., Virtue, P., Nichols, P., 2010. Lipid composition and partitioning of Deepwater chondrichthyans: inferences of feeding ecology and distribution. Mar. Biol. 157 (6), 1367–1384.
Phleger, C.F., 1998. Buoyancy in marine fishes: direct and indirect role of lipids. Am. Zool. 38, 321–330.
Priede, I.G., Froese, R., Bailey, D.M., Bergstad, O.A., Collins, M.A., Dyb, J.E., King, N., 2006. The absence of sharks from abyssal regions of the world's oceans. Proc. R. Soc. Lond. B Biol. Sci. 273 (1592), 1435–1441.
Sargent, J.R., Gatten, R.R., McIntosh, R., 1972. The distribution of neutral lipids in shark tissues. J. Mar. Biol. Assoc. 53, 649.
Sepulveda, C.A., Wegner, N.C., Bernal, D., Graham, J.B., 2005. The red aerobic muscle morphology of the thresher sharks (family Alopiidae). J. Exp. Biol. 208, 4255–4261.
Shadwick, R.E., Goldbogen, J.A., 2012. Muscle function and swimming in sharks. J. Fish Biol. 80, 1904–1939.
Shadwick, R.E., Farrell, A.P., Brauner, C.J., 2016. Physiology of Elasmobranch Fishes: Structure and Interaction with Environment. 34A Elsevier.
Socrates, G., 2001. Infrared and Raman Characteristic Group Frequencies, 3rd ed. J. Sons, West Sussex.
Syme, D.A., 2005. Functional properties of skeletal muscle. Fish Physiol. 23, 179–240.
Tewari, J., Irudayaraj, J., 2004. Quantification of saccharides in multiple floral honeys using fourier transform infrared microattenuated total reflectance spectroscopy. J. Agric. Food Chem. 52 (11), 3237–3243.
Thompson, K.S., Simanek, D.E., 1977. Body form and locomotion in sharks. Amer. Zool. 17, 343–354.
Tiryaki, G.Y., Ayvaz, H., 2017. Quantification of soybean oil adulteration in extra virgin olive oil using portable Raman spectroscopy. J. Food Meas. Charact. 11 (2), 523–529.
Treberg, J.R., Speers-Roesch, B., 2016. Does the physiology of chondrichthyan fishes constrain their distribution in the deep sea? J. Exp. Biol. 219 (5), 615–625.
Treberg, J.R., Martin, R.A., Driedzic, W.R., 2003. Muscle enzyme activities in a deep-sea squaloid shark, Centroscyllium fabricii, compared with its shallow-living relative, Squalus acanthias. J. Exp. Zool. A. Comp. Exp. Biol. 300 (2), 133–139.
Tsujimoto, M., 1916. A highly unsaturated hydrocarbon in shark liver oil. Ind. Eng. Chem. 8 (10), 889–896.
Vermeulen, P.H., Fernández, J.A., Abbas, O., Dardenne, P., Baeten, V., 2015. Origin identification of dried distillers grains with solubles using attenuated total reflection Fourier transform mid-infrared spectroscopy after in situ oil extraction. Food Chem. 189, 19–26.
Watson, R.R., Dickson, K.A., 2015. Enzyme activities support the use of liver lipid-derived ketone bodies as aerobic fuels in muscle tissues of active sharks. Physiol. Biochem. Zool. 74, 273–282.
Wetherbee, B.M., Nichols, P.D., 2000. Lipid composition of the liver oil of deep-sea sharks from the Chatham rise, New Zealand. Comp. Biochem. Physiol. Part B Biochem. Mol. Biol. 125, 511–521.
Yancey, P.H., Speers-Roesch, B., Atchinson, S., Reist, J.D., Majewski, A.R., Treberg, J.R., 2018. Osmolyte adjustments as a pressure adaptation in deep-sea chondrichthyan fishes: an intraspecific test in arctic skates (Amblyraja hyperborea) along a depth gradient. Physiol. Biochem. Zool. 91 (2), 788–796.